Geopolymer Synthesis Using Garnet Tailings from Molybdenum Mines

An Wang [1,2], Hongzhao Liu [1,*], Xiaofei Hao [1,2], Yang Wang [2], Xueqin Liu [2] and Zhen Li [2,*]

[1] National Research Center of Multipurpose Utilization of Non-metallic Mineral Resources, Zhengzhou 450006, China; charilie@126.com (A.W.); haopaper@163.com (X.H.)

[2] Engineering Research Center of Nano-Geomaterials of Ministry of Education, Faculty of Materials Science and Chemistry, China University of Geosciences, Wuhan 430074, China; ywangcug@hotmail.com (Y.W.); liuxq@cug.edu.cn (X.L.)

[*] Correspondence: hongzhao99@126.com (H.L.); zhenli@cug.edu.cn (Z.L.); Tel.: +86-027-67883737 (Z.L.)

check for updates

Abstract: Garnet tailings obtained in large quantities from molybdenum ore beneficiation are regarded as industrial waste, which not only occupies large areas of land but also causes environmental issues and ecological fines. Preparing garnet tailings based geopolymers (GTGs) is one of the efficient methods to recycle and utilize garnet mine tailings. In this work, geopolymers were synthesized using garnet tailing (GT) and metakaolin (MK) as the main precursors and sodium silicate as the alkali-activation agent. The effect of MK and alkali activator dosage, as well as curing temperature on the compression strength of GTGs were analyzed in detail. Results showed that the maximum strength (46 MPa, 3 days) was reached at a 20 wt % MK dosage with 35% sodium silicate addition cured at room temperature. The microstructure and phase composition of GTGs were investigated by X-ray diffraction (XRD), scanning electron microscopy (SEM), and Fourier-transform infrared spectroscopy (FTIR), which confirmed the formation of an amorphous geopolymer gel. Lastly, it can be concluded that the garnet tailing is a promising material for geopolymer production, as an alternative for its utilization.

1. Introduction

Mine tailing is mineral waste produced by the beneficiation process of ore (washing and flotation). A series of problems appear from the storage and disposal of mine tailing, such as the occupation of large areas of land, contamination of surface and underground water by toxic metal leachates, as well as air pollution due to dust emissions [1–4]. Large quantities of mine tailings were produced during the last few decades in China, due to the rapid development of the mining industry. These tailings become a major concern in the mining industry. In current practice, the most common method to manage them is disposal in landfills, which requires costly construction and maintenance [5–9]. That is why cost-effective and sustainable alternatives are urgently required.

Geopolymers are a new type of aluminosilicates with a three-dimensional (3D) amorphous or semi-crystalline micro-structure, which exhibit several important properties such as excellent mechanical properties, chemical and thermal stabilities, low cost and are environmentally friendly due to the low CO_2 emission during preparation process [10–14]. These characteristics mentioned above make geopolymers have a potential application in construction materials, thermal insulator and surface capping. In general, geopolymers are produced by mixing an aluminosilicate reactive material such as metakaolin or fly ash (FA) with strong alkali solutions at room or slightly higher temperatures. After mixing, the alkali activator dissolves the solid aluminosilicate source and aluminate and silicate monomers are formed which immediately undergo a polycondensation reaction to a dissolved

crosslink species of sodium aluminosilicate. By further polycondensation reaction, a three-dimensional aluminosilicate gel is formed resulting in a solid material [15]. Therefore, the geopolymer synthesis process can be divided into two periods: dissolution-hydrolysis and hydrolysis-polycondensation. However, once the aluminosilicate material is mixed with the activator solution, these two steps may occur simultaneously [16]. Consequently, some natural minerals or mine tailings that have a rich silico-aluminate composition are a potential resource for the fabrication of geopolymers [17–19]. During the past two decades, there has been an increasing number of studies on the fabrication of geopolymers using mine tailings as the main sources, such as iron ore tailing [20,21], volcanic ash [22–24], red mud [25], fly ash [26–28], phosphate sludge [29,30] and vanadium tailings [31,32].

Garnet tailing (GT) is one of the main mining and mineral wastes produced by molybdenum ore beneficiation [33,34]. According to Reference [9], several million tons of garnet was imported in Malaysian in 2013 and most of it was dumped as wastes. The main compositions of GT are silicon, aluminum and iron oxides, which make it a suitable mineral source for the preparation of geopolymers. Additionally, the contamination risk of iron ions could be effectively solved due to the effective stabilization effect of heavy metals by geopolymers. In addition, garnet has good wear resistance, which guarantees a long service life of garnet-based geopolymers. Until now, many mine tailings have been used to the production of geopolymers. However, the research about the reuse of GT as raw material for the preparation of geopolymers has not been reported.

Herein, our primary objective is to investigate the feasibility of geopolymer synthesis using GT as the main aluminosilicate source material. First, the effects of MK and sodium silicate dosage, as well as the curing temperature on the compressive strength of GTGs, were investigated. Then, the phases and microstructure transformations during the geopolymerization process were analyzed by XRD, SEM and FTIR.

2. Materials and Methods

2.1. Raw Materials

The studied GT was obtained in the form of dry powder from a molybdenum mine in Luanchuan, China. The chemical composition of the GT is largely composed of SiO_2 (44.28%), Al_2O_3 (5.57%), Fe_2O_3 (13.82%), and CaO (30.26%), along with some trace elements, as shown in Table 1.

Table 1. The main chemical constituents of garnet and metakaolin.

Components (wt %)	SiO_2	Al_2O_3	Fe_2O_3	CaO	MgO	Na_2O	K_2O
MK	53.56	43.92	1.08	0.14	0.10	0	0.78
GT	44.28	5.57	13.82	30.26	0.81	0.23	0.13

The morphological and mineralogical characterization of the raw materials (MK and GT) are shown in Figures 1 and 2. It can be observed from Figure 1 that the mineral composition of the garnet tailing is quartz, calcite, calcium aluminum garnet phase, iron aluminum garnet and calcium iron garnet, while the only crystalline phase in metakaolin is a small amount of quartz. From the SEM images in Figure 2, the garnet is composed of lots of small sheet-shape particles with many pores on the surface, while the metakaolin exhibits relatively large sheet-like particles. A commercial metakaolin (MK) was used to adjust the Si/Al ratio of raw materials due to the relatively low content of Al in GT. The chemical composition of MK is also given in Table 1.
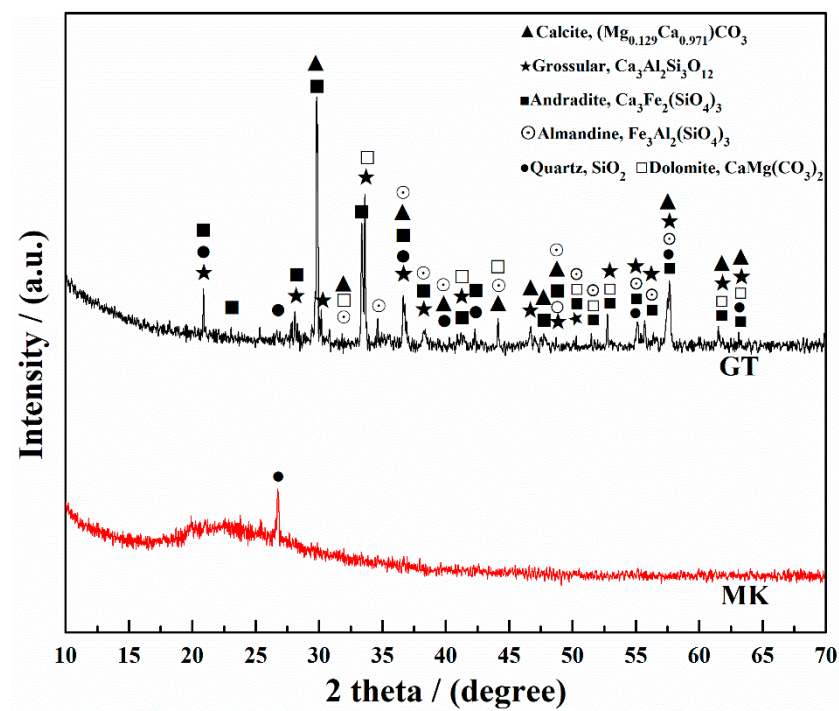
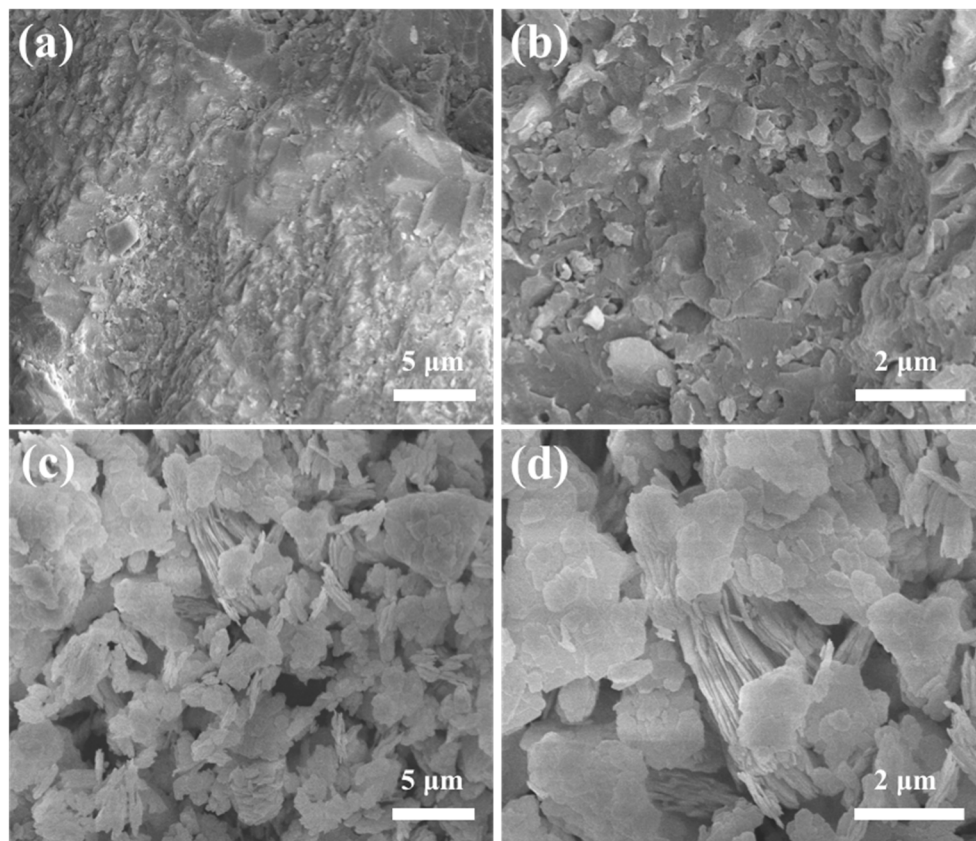**Figure 1.** The XRD patterns of the garnet tailing and metakaolin.

Figure 2. The morphology of the garnet (**a**,**b**) and metakaolin (**c**,**d**).

2.2. Geopolymer Synthesis

Geopolymers were produced using GT as the main raw material mixed with 0, 10, 20, 30, and 100 wt % of MK with respect to the mass of the total solid, and activated by sodium silicate solution with a modulus of 1.5. The MK was obtained by calcining kaolin from Guangdong province, China, calcined at 800 °C for 6 h in a muffle furnace, and cooled naturally in the furnace to room temperature. A sodium silicate solution purchased from Zhongfa company in Guangdong province, China was used as alkali activator. The molar ratio SiO_2 to Na_2O of the sodium silicate solution was adjusted by sodium hydroxide (Sigma Aldrich, St. Louis, MO, USA, minimum purity 98%) from 3.1 to 1.5. The GT samples with 0, 10, 20, 30 and 100 wt % MK in the synthesis process were named as GTGs-0, GTGs-1, GTGs-2, GTGs-3 and GTGs-4, respectively. The details of the amount of the raw materials are listed in Table 2. Typically, GT and MK were mixed together for 10 min, and then a sodium silicate solution was added, followed by another 10 min of mixing. The mixtures were cast in cubic PVC molds (50 mm × 50 mm × 50 mm) and shaken for 5 min to remove the air bubbles in the paste. After that, the molds were placed to cure at different temperatures for different duration days. Here, the effects of the dosage of MK, the amount of sodium silicate and the curing temperature on the compressive strength of geopolymer have been studied in detail.

Table 2. The details of the number of raw materials for the geopolymers preparation.

Samples	Garnet/g	Metakaolin/g	Sodium Silicate/g	Water/g
GTGs-0	600	0		30
GTGs-1	540	60	180	40
GTGs-2	480	120		60
GTGs-3	420	180		80

2.3. Characterization

The compressive strength tests of products produced at various conditions were conducted by an EHC-1300 mechanical tester from Xingao Technology, Gaoyao City, Guangdong, China. For each test, five cubic samples were tested with the experimental values being averaged. The phase compositions, micro/nanostructure and morphology of raw mineral materials and geopolymer samples were characterized using X-ray diffraction collected from 10° to 70°, 2°/min (XRD, Bruker AXS D8 Advance (Bruker, Billerica, MA, USA), CuKα-radiation produced at 40 KV and 40 mA, λ = 1.540598 Å), field-emission scanning electron microscopy operating at an accelerating voltage of 10 kV (SU8010, FESEM, Hitachi, Tokyo, Japan,) and Fourier-transform infrared (FTIR, Nexus 670, Thermo Nicolet, MA, USA) spectroscopy with wavelengths from 600 to 4000 cm^{-1}, respectively.

To determine the total contents of active Al_2O_3 and SiO_2 in the raw materials GT and MK, alkaline leaching tests were conducted in a 5 M sodium hydroxide solution, with a solid/liquid mass ratio of 1:100, in a rotary agitator at 25 ± 2 °C for 18 h. After the leaching tests, samples were filtered through 0.45 μm filter membranes, and then the concentrations of Al and Si in the filtrates were determined by Inductively Coupled Plasma-Optical Emission Spectrometry (ICP-OES) using Optima8300DV (Perkin Elmer, Waltham, MA, USA) [35]. The dissolution efficiencies of Al_2O_3 and SiO_2 in alkaline leaching tests were calculated using Equation (1) below:

$$\text{Dissolution efficiency (wt\%)} = \frac{\text{The mass of } Al_2O_3 \text{ or } SiO_2 \text{ in the filtraten}}{\text{The mass of } Al_2O_3 \text{ or } SiO_2 \text{ in the raw materials}} \tag{1}$$

3. Results

3.1. Transformations of Soluble Al and Si

The dissolution of Al and Si components from the raw materials GT and MK were measured by the solubility test in a 5 M NaOH solution, as shown in Figure 3. Obviously, the MK solubility in

sodium hydroxide solution is much higher than that of GT dissolution, which is attributed to the heat treatment of MK at 800 °C. The dissolution efficiencies of Al_2O_3 and SiO_2 in the MK are more than 70% and 50%, respectively. The high solubility of MK is due to its amorphous characteristic. However, the dissolution efficiencies of Al_2O_3 and SiO_2 in GT are all below 2%, which is consistent with the low compressive strength of GTGs-0 in the early stage. From this result, it can be known that garnet is an inert material and unreactive in alkaline. Therefore, it is necessary to increase the reactivity of GT by adding a certain amount of high activity MK in the process of geopolymer synthesis.
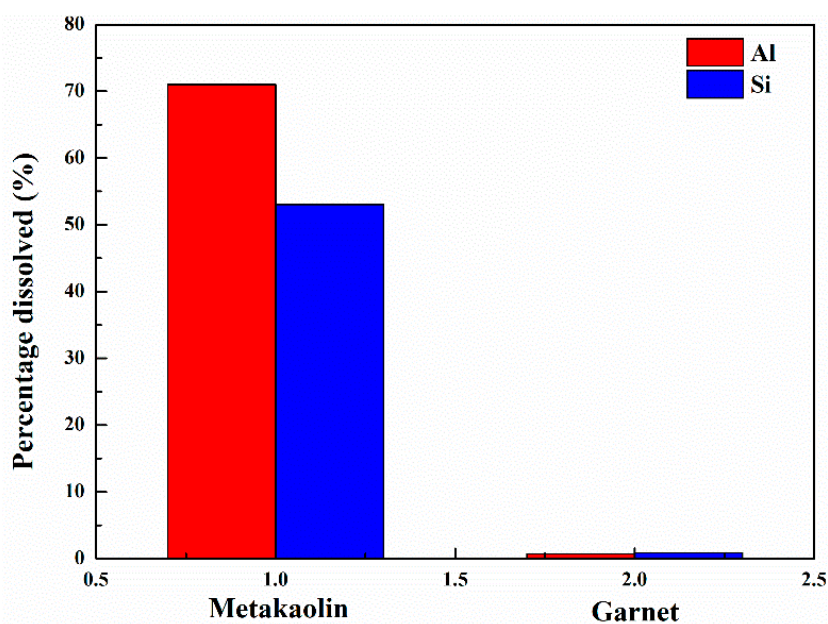

Figure 3. The dissolution efficiency of Al_2O_3 and SiO_2 in the alkaline media test of raw garnet tailing and metakaolin.

3.2. Compressive Strength Test

The influence of the MK dosage, the amount of sodium silicate addition and curing temperature on the compressive strength of GTGs were investigated, as shown in Figure 4. The compressive strength of GTGs containing MK at 10, 20 and 30 wt % cured for 3 days at 60 °C with 30% sodium silicate addition is presented in Figure 4a. As a reference, the compressive strength of geopolymers prepared by pure GT and MK were also tested. Obviously, a less than 2 MPa compressive strength was achieved for the GTGs-0 without the addition of MK, indicating that the strength of GTGs was not developed at the early stages without the help of MK [36–41]. When MK is added, the compressive strength of GTGs increases first and then decreases with the increase of MK content. When the MK content increases from 0 to 20%, the compressive strength of GTGs significantly increases, because of that the high activity of MK greatly enhances the geopolymerization degree of GTGs. While there has been a decline in compressive strength of GTGs when the MK dosage increases from 20% to 30%, this is because that the amount of active Al and Si components in the GTGs-2 sample reaches the optimal ratio. When the amount of MK continues to increase, the ratio of silicon to aluminum in the sample is unbalanced, resulting in a decrease of the reaction degree and compressive strength of GTGs.

Figure 4b shows the compressive strength of GTGs-2 with 20%, 25%, 30%, 35%, 40% sodium silicate addition after 3 days curing at 60 °C, respectively. As seen with an increase in the sodium silicate addition, the compressive strength of the samples increases first and then decreases. The maximum strength 36 MPa is achieved with 35% sodium silicate.
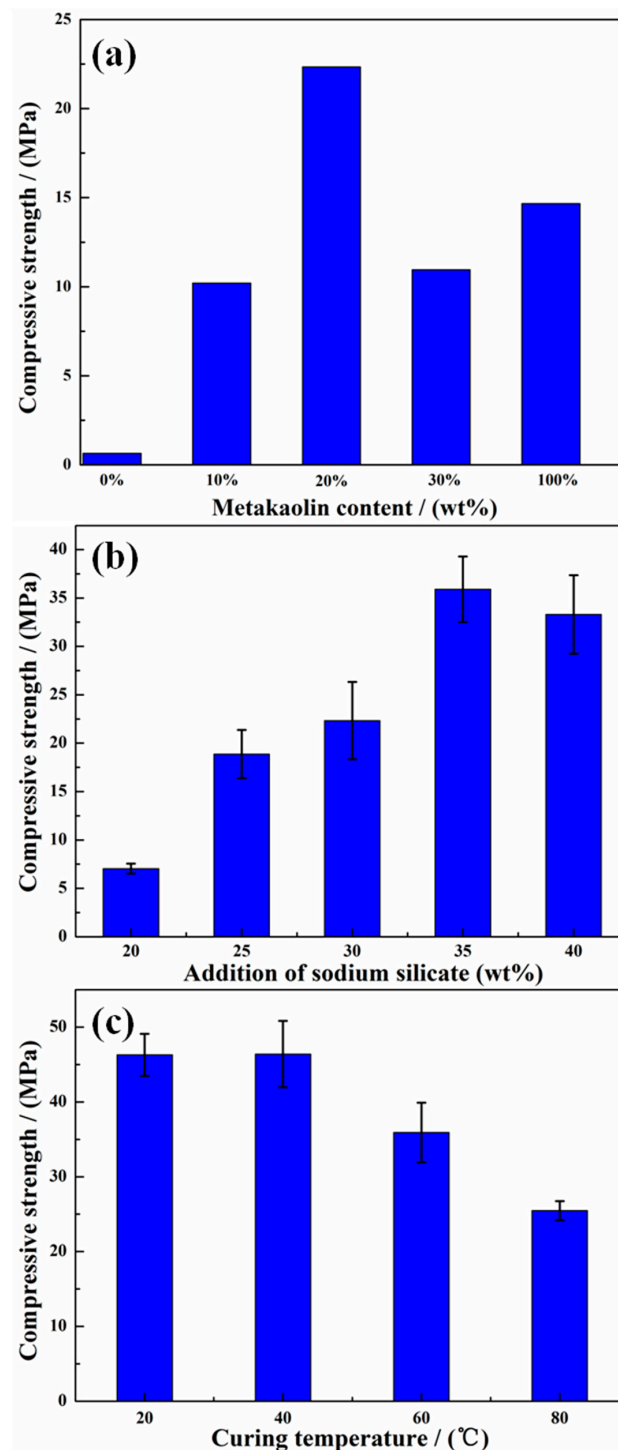
Figure 4. The compressive strength test results of samples with different metakaolin content cured for 3 days at 60 °C with 30% sodium silicate addition (**a**), under different sodium silicate additions cured for 3 days at 60 °C with 20% metakaolin content (**b**) and under different curing temperature for 3 days with 20% metakaolin content and 30% sodium silicate addition (**c**).

During the geopolymerization reaction, one of the most important functions of the alkali activator is to accelerate the dissolution of Si and Al component from GT and MK. It means the Si/Al ratio in the chemical reaction is adjusted by the dosage of alkali activator. As a result, an excessive sodium silicate addition would destroy the optimal Si/Al ratio, resulting in a decrease of compressive strength [42]. Figure 4c presents the influence of curing temperature on the compressive strength of GTGs-2 prepared

with 35% sodium silicate addition after 3 days of curing. It is clear that the increase in curing temperature has a negative effect on strength. At ambient temperatures (20 and 40 °C), the compressive strength (above 45 MPa) is the highest for all the GT-based geopolymers of the study, indicating that the GTGs has the optimal mechanical property under normal temperature conditions. As the curing temperature increases, lots of pores are produced at a relatively high temperature, resulting in low density and compressive strength of the obtained geopolymers [43].

3.3. X-Ray Diffraction Results

To investigate the mechanism of GT and MK on the formation of geopolymer, XRD patterns of samples with different MK content and curing time are shown in Figure 5. The XRD patterns of GTGs-0 display peaks due to grossular, andradite, dolomite, calcite and quartz, and other crystalline phases such as almandine and boehmite are also detected. The grossular, andradite and almandine phases belong to the garnet phase. From the mineral phase analysis of GT and GTGs-0 shown in Figure 5a, we can see that the relative content of the mineral phase in GTGs-0 has changed greatly with the increase of curing time. The almandine phase belonged to garnet completely disappeared in GTGs-0 after curing for 3 days. Additionally, the diffraction peaks intensity of other garnet phase decreased significantly, indicating that the garnet phase could be dissolved in sodium silicate and participated in the geopolymerization process. After curing for 28 days, the garnet phase diffraction peak of GTGs-0 decreases slowly, while the intensity of the diffraction peak and content of the quartz phase decreases significantly, indicating that the alkali activator reacts with the quartz phase at this stage. Compared to the GTGs-0, the grossular and quartz crystalline phases intensity of GTGs-2 decrease obviously, indicating that better geopolymerization is induced due to the addition of MK, as shown in Figure 5b. In addition, compared to GTGs-1 and GTGs-3, the diffraction peaks number of the mineral phases (such as boehmite and anhydrite) of the GTGs-2 is significantly reduced. For GTGs-4, only a small peak attributed to quartz at 26° is observed, indicating the good activity of MK components during the geopolymerization under a strongly alkaline environment. There are two reasons to support this point. First, combined with the SEM observation, the particles in the samples gradually decrease and the gelatinous substance in the amorphous structure gradually increases, which is consistent with the disappearance of the phase. Second, the compressive strength of GTGs-1, GTGs-2, GTGs-3 and GTGs-4 are much higher than that of GTGs-0, indicating the better geopolymerization process. Figure 5b illustrates the changes that occurred in the phases of GTGs-2 with different curing times. It obviously demonstrated that by increasing the curing times, the number and intensity of diffraction peaks increase. This may due to that at the initial curing stage, the mineral phase is surrounded by the dissolved silicon-aluminum component, so the participates in the polymerization process, which caused the consumption of active silicon-aluminum component encapsulated mineral phase [44]. Therefore, the intensity of the diffraction peaks increases reasonably.
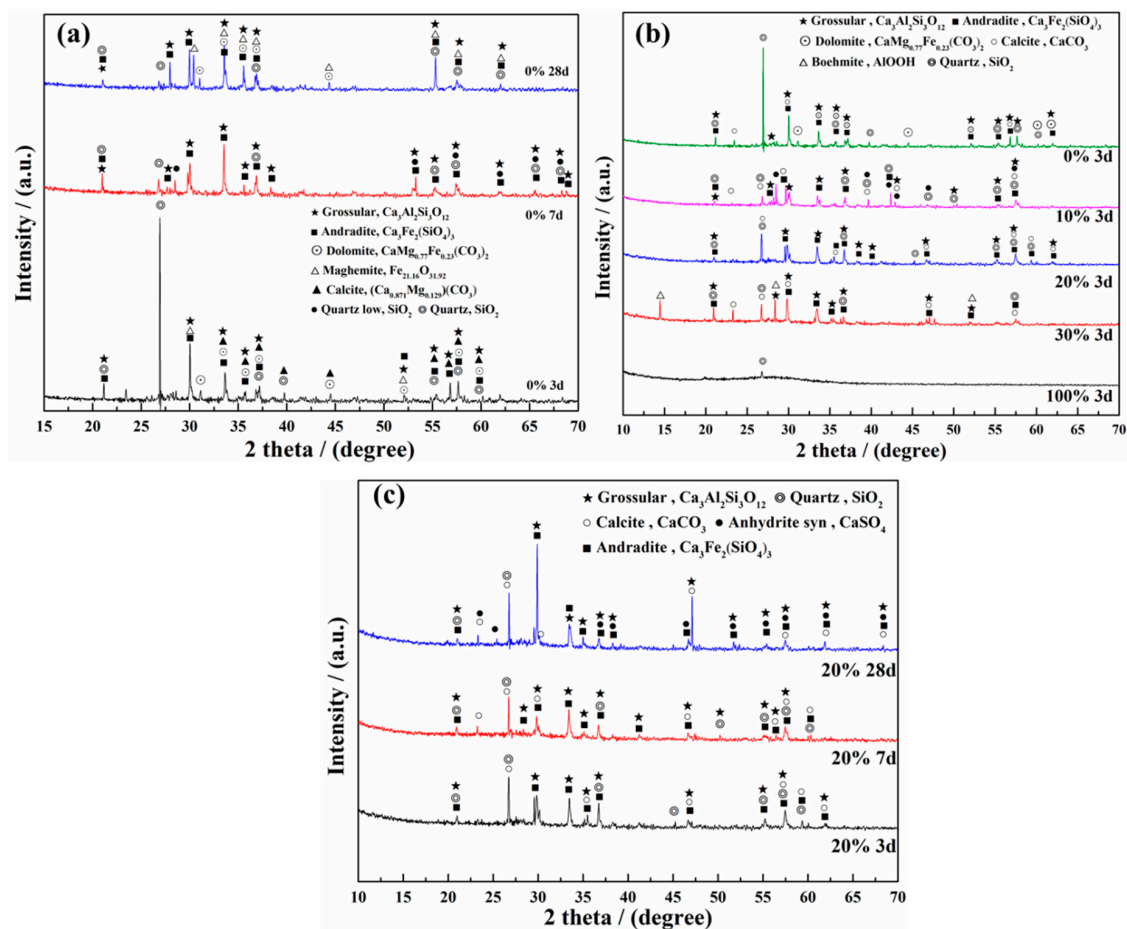
Figure 5. The X-ray diffraction patterns of GTGs-0 after 3, 7, and 28 days of curing (**a**), GTGs-1, GTGs-2 and GTGs-3 for 3 days compared to the GTGs-0 and GTGs-4 (**b**), and GTGs-2 after 3, 7, and 28 days of curing (**c**), respectively.

3.4. Scanning Electron Microscopy (SEM)

The internal microstructure of GTGs-0 and GTGs-2 was identified by SEM images, as shown in Figure 6. Figure 6a–c is the morphology of GTGs-0 cured at 3, 7 and 28 days, showing a typical microstructure of consolidated geopolymer materials. When curing at 3 days, it can be observed from Figure 6a that many particles with a size of about 2 to 5 μm are glued together to form an irregular gelatinous substance in the GT single-component sample. This relatively large size may be because of the undissolved crystalline phase components from the raw materials in the early stage of curing. With increasing curing time, the large-sized substrates originally present in the samples were combined to form a colloidal substance, then solidified into a random three-dimensional crosslinked structure, as shown in Figure 6b,c.

After the addition of MK, the size of gel-like particles is much smaller than that of GTGs-0, indicating that the dissolution rate of the crystal component in raw materials improved greatly with the help of MK, as shown in Figure 6d–f. For 3 days, a large number of amorphous gelatinous substrates are formed in GTGs-2, which are closely packed together to form a dense structure without obvious cracks and holes. After 7 days of curing, some significant cracks appear in the structure. Furthermore, the dense structure formed in the sample is surrounded by a number of unreacted substrates and undissolved large-sized crystal particles in the sample after 28 days of curing. It is worth noting that the structure evolution observed above is consistent with the compressive strength changes of geopolymers prepared at different conditions.
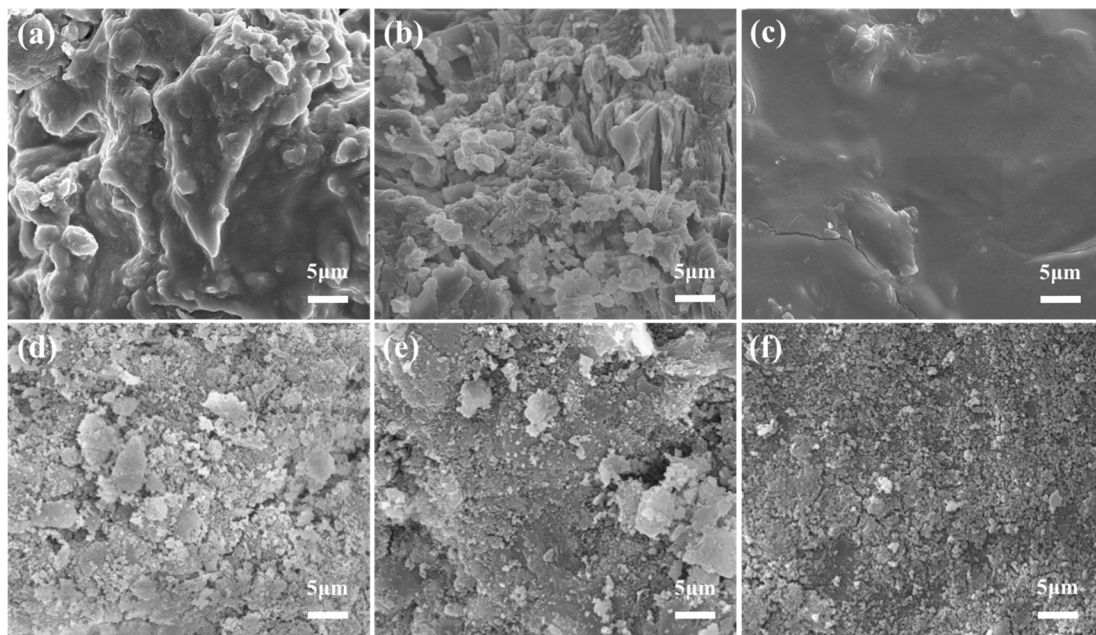
Figure 6. The SEM images of GTGs-0 (**a**–**c**) and GTGs-2 (**d**–**f**) after 3, 7, and 28 days of curing, respectively.

3.5. The FTIR Spectra of Sample

The FTIR spectrum of GTGs-2 was tested to investigate the combination formation of GT and MK in geopolymer gel. As a comparison, the spectra of GTGs-0 is also employed, as shown in Figure 7. Briefly, the spectra of GTGs-0 show that the absorption peaks at 3450 and 1650 cm^{-1} correspond to the O–H group and H–O–H bending vibration peak in water molecules of the sample [45,46], while the vibration band at 1427 and 460 cm^{-1} is the O–Ca–O stretching and Si–O–Al out-of-plane vibration in the raw materials. The peaks at 1000 and 710 cm^{-1} correspond to the Si (Al)–O–Si and Al–O–Si stretching respectively, which are attributed to the asymmetrically stretched aluminosilicate of geopolymer products [31]. In-plane and out-of-plane vibration peaks of Si–O–Al existing at 460 and 550 cm^{-1} indicate that the Al composition is in the form of the [AlO$_6$] octahedron. While the peak at 710 cm^{-1} confirms the existence of the [AlO$_4$] tetrahedron, indicating that the Al component takes part in the geopolymerization process. Due to this, the Al component in garnet tailing is in the form of [AlO$_6$] octahedron. In addition, during the curing process of GTGs-0, the characteristic peak intensity of the [AlO$_4$] tetrahedron at 710 cm^{-1} is enhanced apparently with curing time increasing, further confirmed that GT can react with sodium silicate and not only act as a filler in the final geopolymers. During the geopolymerization process, the [AlO$_6$] octahedron in the garnet tailing is destroyed during the reaction and transformed to the [AlO$_4$] tetrahedron. After the addition of 20% MK, the peak intensity at 3450 and 1650 cm^{-1} decrease apparently, indicating that the amount of free water in the sample significantly decreases. Importantly, the peaks at 1427 and 460 cm^{-1} from the starting materials decrease apparently indicate the activated GT in GTGs-2 is more disordered than that in GTGs-0. Moreover, an increase in the strength of Al–O–Si vibrations at 1000 and 710 cm^{-1} suggests that the degree of polymerization increased in GTGs-2.
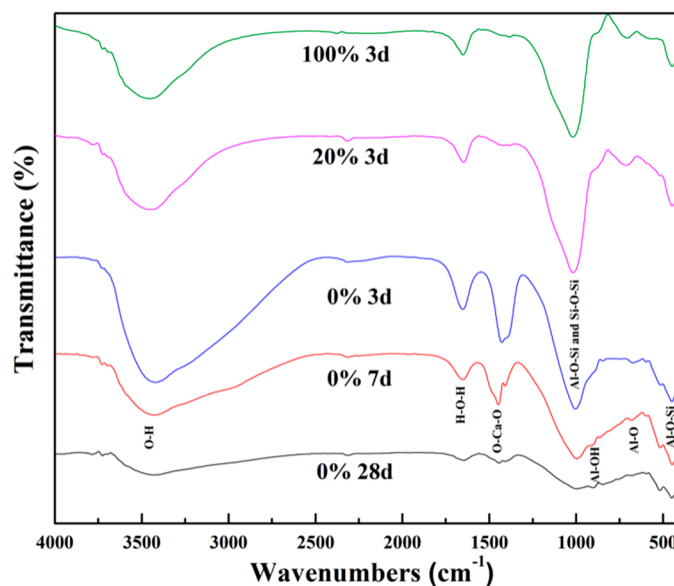
Figure 7. The FTIR spectra of the GTGs-0, GTGs-2 and GTGs-4.

4. Conclusions

In this study, geopolymer was successfully prepared using garnet tailing as a construction material with the addition of metakaolin. The analysis of the results from XRD, SEM and FTIR indicated the formation of amorphous geopolymers. The pure garnet tailings-based geopolymers exhibit a 15 MPa compressive strength, which is much higher than that of geopolymers based on pure vanadium tailing and fly ash. The dependence shown between compressive strength and metakaolin dosage suggested that a one-part geopolymer prepared by pure garnet tailings showed poor strength value, especially in the early stage. The addition of metakaolin played an important role in the improvement of compressive strength, and the geopolymer synthesized at 20% metakaolin addition displayed the highest compressive strength. Additionally, 30% sodium silicate addition was the optimal condition for the compressive strength. The influence of curing temperature on the compressive strength indicated that room temperatures (20 and 40 °C) favored compressive strength. After optimization, GTGs-2 prepared with 35% sodium silicate addition after 3 curing days at room temperature achieved the compressive strength (above 45 MPa). From the results of XRD, it was found that MK had a good activity during the geopolymerization and the calcium component in the GT participated in the polymerization process. From this work, it can be concluded that it is possible to apply garnet tailings to the preparation of geopolymers.

Author Contributions: Z.L., X.L. and H.L. conceived the project; A.W. wrote initial drafts of the work; X.L. and Y.W. wrote the final paper; A.W. and X.H. designed and performed the experiments, and characterized the samples. All authors discussed the results and commented on the manuscript.

References

1. Gitari, W.; Thobakgale, R.; Akinyemi, S. Mobility and Attenuation Dynamics of Potentially Toxic Chemical Species at an Abandoned Copper Mine Tailings Dump. *Minerals* **2018**, *8*, 64. [CrossRef]
2. Xu, D.; Yang, H.; Ouyang, J.; Zhang, Y.; Fu, L.; Chen, D. Lauric Acid Hybridizing Fly Ash Composite for Thermal Energy Storage. *Minerals* **2018**, *8*, 161. [CrossRef]
3. Bian, Z.; Miao, X.; Lei, S.; Chen, S.E.; Wang, W. The challenges of reusing mining and mineral-processing wastes. *Science* **2012**, *337*, 702–703. [CrossRef] [PubMed]

4. Franks, D.M.; Boger, D.V.; Côte, C.M.; Mulligan, D.R. Sustainable development principles for the disposal of mining and mineral processing wastes. *Resour. Policy* **2011**, *36*, 114–122. [CrossRef]

5. Amin, S.K.; El-Sherbiny, S.A.; El-Magd, A.A.M.A.; Belal, A.; Abadir, M.F.; Amin, S.K. Fabrication of geopolymer bricks using ceramic dust waste. *Constr. Build. Mater.* **2017**, *157*, 610–620. [CrossRef]

6. Komnitsas, K.; Zaharaki, D.; Bartzas, G. Effect of sulphate and nitrate anions on heavy metal immobilisation in ferronickel slag geopolymers. *Appl. Clay Sci.* **2013**, *73*, 103–109. [CrossRef]

7. Monosi, S.; Tittarelli, F.; Giosuè, C.; Ruello, M.L. Effect of two different sources and washing treatment on the properties of UFS by-products for mortar and concrete production. *Constr. Build. Mater.* **2013**, *44*, 260–266. [CrossRef]

8. Kinnunen, P.; Ismailov, A.; Solismaa, S.; Sreenivasan, H.; Räisänen, M.L.; Levänen, E.; Illikainen, M. Recycling mine tailings in chemically bonded ceramics—A review. *J Clean. Prod.* **2018**, *174*, 634–649. [CrossRef]

9. Muttashar, H.L.; Hussin, M.W.; Ariffin, M.A.M. Realisation of enhanced self-compacting geopolymer concrete using spent garnet as sand replacement. *Mag. Concr. Res.* **2017**, *70*, 558–569. [CrossRef]

10. Dimas, D.D.; Giannopoulou, I.P.; Panias, D. Utilization of Alumina Red Mud for Synthesis of Inorganic Polymeric Materials. *Min. Proc. Ext. Met. Rev.* **2009**, *30*, 211–239. [CrossRef]

11. Nikolov, A.; Rostovsky, I.; Nugteren, H. Geopolymer materials based on natural zeolite. *Case Stud. Constr. Mater.* **2017**, *6*, 198–205. [CrossRef]

12. Villa, C.; Pecina, E.T.; Torres, R.; Gómez, L. Geopolymer synthesis using alkaline activation of natural zeolite. *Constr. Build. Mater.* **2010**, *24*, 2084–2090. [CrossRef]

13. Song, L.; Li, Z.; Duan, P.; Huang, M.; Hao, X.; Yu, Y. Novel low cost and durable rapid-repair material derived from industrial and agricultural by-products. *Ceram. Int.* **2017**, *43*, 14511–14516. [CrossRef]

14. Davidovits, J. Geopolymers: Inorganic polymeric new materials. *J. Therm. Anal. Calorim.* **1991**, *37*, 1633–1656. [CrossRef]

15. Ranjbar, N.; Kuenzel, C. Influence of preheating of fly ash precursors to produce geopolymers. *J. Am. Ceram. Soc.* **2017**, *100*, 3165–3174. [CrossRef]

16. Ranjbar, N.; Mehrali, M.; Behnia, A.; Alengaram, U.J.; Jumaat, M.Z. Compressive strength and microstructural analysis of fly ash/palm oil fuel ash based geopolymer mortar. *Mater. Des.* **2014**, *59*, 532–539. [CrossRef]

17. Duxson, P.; Mallicoat, S.W.; Lukey, G.C. The effect of alkali and Si/Al ratio on the development of mechanical properties of metakaolin-based geopolymers. *Colloids Surf. A Physicochem. Eng. Asp.* **2007**, *292*, 8–20. [CrossRef]

18. Glid, M.; Sobrados, I.; Rhaiem, H.B.; Sanz, J.; Amara, A.B.H. Alkaline activation of metakaolinite-silica mixtures: Role of dissolved silica concentration on the formation of geopolymers. *Ceram. Int.* **2017**, *43*, 12641–12650. [CrossRef]

19. Sabbatini, A.; Vidal, L.; Pettinari, C.; Sobrados, I.; Rossignol, S. Control of shaping and thermal resistance of metakaolin-based geopolymers. *Mater. Des.* **2017**, *116*, 374–385. [CrossRef]

20. Duan, P.; Yan, C.J.; Zhou, W.; Ren, D. Fresh properties, compressive strength and microstructure of fly ash geopolymer paste blended with iron ore tailing under thermal cycle. *Constr. Build. Mater.* **2016**, *118*, 76–88. [CrossRef]

21. Duan, P.; Yan, C.J.; Zhou, W.; Ren, D. Development of fly ash and iron ore tailing based porous geopolymer for removal of Cu(II) from wastewater. *Ceram. Int.* **2016**, *42*, 13507–13518. [CrossRef]

22. Pooria, G.; Navid, R. Clayey soil stabilization using geopolymer and portland cement. *Constr. Build. Mater.* **2018**, *188*, 361–371.

23. Djobo, J.N.Y.; Tchakouté; Kouamo, H.; Ranjbar, N.; Elimbi, A.; Tchadjié, L.N.; Njopwouo, D. Gel composition and strength properties of alkali-activated oyster shell-volcanic ash: Effect of synthesis conditions. *J Am. Ceram. Soc.* **2016**, *188*, 361–371. [CrossRef]

24. Ranjbar, N.; Kashefi, A.; Maheri, M.R. Hot-pressed geopolymer: Dual effects of heat and curing time. *Cem. Concr. Comp.* **2018**, *86*, 1–8. [CrossRef]

25. Ye, N.; Chen, Y.; Yang, J.; Liang, S.; Hu, Y.; Hu, J.; Zhu, S.; Fan, W.; Xiao, B. Transformations of Na, Al, Si and Fe species in red mud during synthesis of one-part geopolymers. *Cem. Concr. Res.* **2017**, *101*, 123–130. [CrossRef]

26. Fernández-Jiménez, A.; Palomo, A.; Criado, M. Microstructure development of alkali-activated fly ash cement: A descriptive model. *Cem. Concr. Res.* **2005**, *35*, 1204–1209. [CrossRef]

27. Rosas-Casarez, C.A.; Arredondo-Rea, S.P.; Cruz-Enríquez, A.; Corral-Higuera, R.; Gómez-Soberón, J.M.; Medina-Serna, T.D.J. Influence of Size Reduction of Fly Ash Particles by Grinding on the Chemical Properties of Geopolymers. *Appl. Sci.* **2018**, *8*, 365. [CrossRef]

28. Toniolo, N.; Boccaccini, A.R.; Toniolo, N.; Boccaccini, A.R. Fly ash-based geopolymers containing added silicate waste: A review. *Ceram. Int.* **2017**, *43*, 14545–14551. [CrossRef]

29. Moukannaa, S.; Loutou, M.; Benzaazoua, M. Recycling of phosphate mine tailings for the production of geopolymers. *J. Clean. Prod.* **2018**, *185*, 891–903. [CrossRef]

30. Dabbebi, R.; de Aguiar, J.L.B.; Camões, A.; Samet, B.; Baklouti, S. Effect of the calcinations temperatures of phosphate washing waste on the structural and mechanical properties of geopolymeric mortar. *Constr. Build. Mater.* **2018**, *185*, 489–498. [CrossRef]

31. Wei, B.; Zhang, Y.; Bao, S. Preparation of geopolymers from vanadium tailings by mechanical activation. *Constr. Build. Mater.* **2017**, *145*, 236–242. [CrossRef]

32. Jiao, X.; Zhang, Y.; Chen, T. Thermal stability of a silica-rich vanadium tailing based geopolymer. *Constr. Build. Mater.* **2013**, *38*, 43–47. [CrossRef]

33. Muttashar, H.L.; Ariffin, M.A.M.; Hussein, M.N.; Hussin, M.W.; Ishaq, S.B. Self-compacting geopolymer concrete with spend garnet as sand replacement. *J. Build. Eng.* **2018**, *15*, 85–94. [CrossRef]

34. Muttashar, H.L.; Ali, N.B.; Ariffin, M.A.M.; Hussin, M.W. Microstructures and physical properties of waste garnets as a promising construction materials. *Case Stud. Constr. Mater.* **2018**, *8*, 87–96. [CrossRef]

35. Ye, N.; Yang, J.; Ke, X.; Zhu, J.; Li, Y.; Xiang, C.; Wang, H.; Li, L.; Xiao, B. Synthesis and characterization of geopolymer from Bayer red mud with thermal pretreatment. *J. Am. Ceram. Soc.* **2014**, *97*, 1652–1660. [CrossRef]

36. Fernández, R.; Ruiz, AI.; Cuevas, J. Formation of CASH phases from the interaction between concrete or cement and bentonite. *Clay Miner.* **2016**, *51*, 223–235. [CrossRef]

37. Mijarsh, M.J.; Johari, M.M.; Ahmad, Z.A. Effect of delay time and Na_2SiO_3 concentrations on compressive strength development of geopolymer mortar synthesized from TPOFA. *Constr. Build Mater.* **2015**, *1*, 64–74. [CrossRef]

38. García-Lodeiro, I.; Fernández-Jiménez, A.; Palomo, A. Variation in hybrid cements over time. Alkaline activation of fly ash–Portland cement blends. *Cem. Concr. Res.* **2013**, *52*, 112–122. [CrossRef]

39. Onisei, S.; Pontikes, Y.; Van Gerven, T.; Angelopoulos, G.N.; Velea, T.; Predica, V. Synthesis of inorganic polymers using fly ash and primary lead slag. *J. Hazard. Mater.* **2012**, *9*, 101–110. [CrossRef]

40. Zhang, L.Y.; Zhang, F.; Liu, M.; Hu, X. Novel sustainable geopolymer based syntactic foams: An eco-friendly alternative to polymer based syntactic foams. *Chem. Eng. J.* **2017**, *313*, 74–82. [CrossRef]

41. Provis, J.L.; Palomo, A.; Shi, C. Advances in understanding alkali-activated materials. *Cem. Concr. Res.* **2015**, *78*, 110–125. [CrossRef]

42. Sun, S.; Lin, J.; Zhang, P.; Fang, L.; Ma, R.; Quan, Z. Geopolymer synthetized from sludge residue pretreated by the wet alkalinizing method: Compressive strength and immobilization efficiency of heavy metal. *Constr. Build. Mater.* **2018**, *170*, 619–626. [CrossRef]

43. Fardjaoui, N.E.H.; Wicklein, B.; Aranda, P. Modulation of inorganic matrices for functional nanoarchitectures fabrication: The simultaneous effect of moisture and temperature in the preparation of metakaolin based geopolymers. *Bull. Chem. Soc. Jpn.* **2018**, *91*, 1158–1167. [CrossRef]

44. Provis, J.; van Deventer, J.S.J. *Alkali-Activated Materials: State-of-the-Art Report*; RILEM TC. 224-AAM; Springer/RILEM: Dordrecht, The Netherlands, 2014; p. 126.

45. Wan, Q.; Rao, F.; Song, S.; Cholico-González, D.F.; Ortiz, N.L. Combination formation in the reinforcement of metakaolin geopolymers with quartz sand. *Cem. Concr. Comp.* **2017**, *80*, 115–122. [CrossRef]

46. Król, M.; Minkiewicz, J.; Mozgawa, W. IR spectroscopy studies of zeolites in geopolymeric materials derived from kaolinite. *J. Mol. Struct.* **2016**, *1126*, 200–206. [CrossRef]